Experimental Neurology xxx (xxxx) xxx

Contents lists available at ScienceDirect

Experimental Neurology

journal homepage: www.elsevier.com/locate/yexnr

Research paper

Spectral and spatial distribution of subthalamic beta peak activity in Parkinson's disease patients

Natasha Darcy [a,b,*], Roxanne Lofredi [a,b], Bassam Al-Fatly [a], Wolf-Julian Neumann [a,c], Julius Hübl [a], Christof Brücke [a], Patricia Krause [a], Gerd-Helge Schneider [d], Andrea Kühn [a,c,e,f,g]

[a] Department of Neurology, Charité - Universitätsmedizin Berlin, Berlin, Germany
[b] Berlin Institute of Health (BIH), Berlin, Germany
[c] Bernstein Center for Computational Neuroscience, Humboldt-Universität, Berlin, Germany
[d] Department of Neurosurgery, Charité - Universitätsmedizin Berlin, Berlin, Germany
[e] NeuroCure, Exzellenzcluster, Charité - Universitätsmedizin Berlin, Berlin, Germany
[f] DZNE, German center for neurodegenerative diseases, Berlin, Germany
[g] Berlin School of Mind and Brain, Humboldt-Universität zu Berlin, Germany

ARTICLE INFO

Keywords:
Parkinson's disease
beta activity
beta peak
Deep brain stimulation
STN
DBS
Adaptive DBS

ABSTRACT

Current efforts to optimise subthalamic deep brain stimulation in Parkinson's disease patients aim to harness local oscillatory activity in the beta frequency range (13–35 Hz) as a feedback-signal for demand-based adaptive stimulation paradigms. A high prevalence of beta peak activity is prerequisite for this approach to become routine clinical practice. In a large dataset of postoperative rest recordings from 106 patients we quantified occurrence and identified determinants of spectral peaks in the alpha, low and high beta bands. At least one peak in beta band occurred in 92% of patients and 84% of hemispheres off medication, irrespective of demographic parameters, clinical subtype or motor symptom severity. Distance to previously described clinical sweet spot was significantly related both to beta peak occurrence and to spectral power (rho −0.21, p 0.006), particularly in the high beta band. Electrophysiological landscapes of our cohort's dataset in normalised space showed divergent heatmaps for alpha and beta but found similar regions for low and high beta frequency bands. We discuss potential ramifications for clinicians' programming decisions. In summary, this report provides robust evidence that spectral peaks in beta frequency range can be detected in the vast majority of Parkinsonian subthalamic nuclei, increasing confidence in the broad applicability of beta-guided deep brain stimulation.

1. Introduction

Deep brain stimulation (DBS) as an established treatment for Parkinson's disease (PD) continues to evolve with major advancements on the verge of routine clinical application. First and foremost, adaptive deep brain stimulation (aDBS) has proven effective in numerous PD cohorts when compared to standard treatment i.e. continuous DBS, lowering total energy delivered to the tissue (TEED) and DBS-associated side effects (Arlotti et al., 2018; Little et al., 2013; Prenassi et al., 2021; Rosa et al., 2017). Though various biomarkers, methods of sensing and stimulating in movement disorders and beyond continue to evolve rapidly (reviewed in Guidetti et al., 2021; Hoang et al., 2017; Krauss et al., 2021), the most studied biomarker so far is activity in the beta frequency band (13–35 Hz) recorded from the subthalamic nucleus in PD patients. Current efforts employ novel devices which record and stimulate simultaneously, tracking local STN beta activity as a real-time marker of symptom severity to adaptively regulate electrical stimulation in a closed loop (Bronte-Stewart et al., 2020). Several past and ongoing studies and clinical trials are now applying aDBS both inside (Piña-Fuentes et al., 2020; Velisar et al., 2019) and outside (Gilron et al., 2021; Kühn et al., 2020; Marceglia et al., 2022; Nakajima et al., 2021) laboratory settings, hoping to optimise adaptive algorithms for patients going about their everyday lives.

To provide some background, beta activity within the basal ganglia network is found both in the physiological state as well as the diseased, with beta synchrony suppressed during movement (Cassidy et al., 2002; Deffains et al., 2018; Kühn et al., 2004). A large body of evidence converges on pathological beta enhancement within STN and across the

* Corresponding author at: Department of Neurology, Charité - Universitätsmedizin Berlin, Berlin, Germany.
E-mail address: natasha.darcy@charite.de (N. Darcy).

https://doi.org/10.1016/j.expneurol.2022.114150
Received 31 January 2022; Received in revised form 27 May 2022; Accepted 15 June 2022
Available online 19 June 2022

cortico-basal ganglia network as a marker for the Parkinsonian (dopamine-depleted) motor state (Brown, 2003; Neumann et al., 2016; Priori et al., 2004; Sharott et al., 2014). More recent work suggests that the pathological nature is characterised by extended durations of beta bursts (Deffains et al., 2018; Lofredi et al., 2019; Tinkhauser et al., 2017). With effective therapeutics, neuromodulation or medication, symptoms and beta activity are suppressed (Anderson et al., 2020; Kühn et al., 2009; Kühn et al., 2008; Kühn et al., 2006; Weinberger et al., 2006; Whitmer et al., 2012), whereby symptom improvement is primarily linked to suppression of activity in the lower beta frequency range from ~13–20 Hz (Brown et al., 2001; Oswal et al., 2016; Priori et al., 2004).

Parkinsonian phenomenology varies greatly, even among patients selected for DBS. Elevated beta activity correlates with bradykinesia and rigidity (Kühn et al., 2009; Neumann and Kühn, 2017), potentially unsuitable or differentially modulated (Godinho et al., 2021) in the tremor-dominant subtype. Widespread use of aDBS based on beta peak activity requires a degree of certainty regarding the reliability of this marker in a phenomenological variety of PD patients. Additionally, experience with intraoperative, postoperative and now chronically available electrophysiological data has shown that these spectra are far from homogenous. Apart from individual peak frequencies and spectral power, some individuals afford multiple beta peaks, either at different contacts or even within single channels. Leading devices currently under investigation in major international clinical trials require preselection of patient-specific beta peak frequencies in each individual's power spectrum (Arlotti et al., 2016; Jimenez-Shahed, 2021).

This retrospective study examined postoperatively recorded local field potentials (LFP) of 106 Parkinsonian patients. This was an extended analysis on a previously published cohort (see methods) aiming to assess electrophysiological activity in relation to diverse patient characteristics and particularly the impact of contact localization, i.e. recording site. Our goal was to establish whether this marker was reliable in a large cohort of PD patients. We further compared spatial extent of peak power distribution in our frequency bands of interest in normalised space.

2. Materials and methods

2.1. Patients and surgery

We reviewed archival data from 106 patients with Parkinson's disease (mean age 63 ± 9 years, range 40–85, 42 females) who underwent bilateral implantation of DBS electrodes into STN between 2008 and 2018. The only inclusion criterion was availability of LFP recordings ON and OFF medication at rest in our database. Before recordings, all patients gave written informed consent approved by the local ethics committee, in accordance with the standards of the Declaration of Helsinki. This cohort was previously published for large-scale investigation of beta burst activity and motor impairment in Lofredi et al. (2022). Information on data acquisition and extended clinical details can be found in this article. In short, subtypes were slightly skewed towards the akinetic-rigid type (47%), with 20% classified as tremor-dominant and 33% equivalent. Motor impairment differed significantly OFF and ON medication, with average UPDRS-III OFF scores of 32.7 ± 12.7 points, and ON scores of 18.3 ± 9.3 points ($p = .002$).

2.2. Recordings and signal processing

Bipolar LFP recordings at rest were performed postoperatively, usually within a week of electrode implantation. Macroelectrodes used for bipolar recordings were Medtronic 3389 ($n = 80$, 3 bipolar channels per electrode), Boston Vercise™ cylindrical ($n = 11$; 8 cylindric contacts, 7 bipolar channels per electrode) and Vercise Cartesia™ directional leads ($n = 15$; 8 contacts). Directional electrodes were usually referenced to their lowermost contact, summed and re-referenced offline, thus approximating 2 bipolar channels between adjacent circular contacts, but omitting the lowermost channel. Recordings were performed OFF (at least 12 h since last dose of Levodopa) and ON dopaminergic medication. In two patients, data was available in only one hemisphere. Details on recording setup and preprocessing can be found in in Lofredi et al. (2022). Briefly, segments free of recording artefacts were identified and low- (98 Hz), high-pass (5 Hz) and notch-filtered (48–52 Hz) and transferred into frequency domain with Morlet wavelets (10 cycles) with a temporal resolution of 200 Hz. LFP recordings were analysed using custom code (MATLAB. (2021). *Version 9.10.0.1684407 (R2021a)*. Natick, Massachussets: The MathWorks Inc.) via SPM (http://www.fil.ion.ucl.ac.uk/spm/) and Fieldtrip (Oostenveld et al., 2011).

As in previous studies (Neumann et al., 2016), resulting power spectra were divided by their total sum across 1-100 Hz. Values thus represent relative power values, which are more comparable between patients. We analysed 658 STN-LFP-channels from 106 patients with Parkinson's disease OFF and 651 ON medication. Highest peaks in alpha (8–12 Hz), low (LBeta, 13–20 Hz) and high beta (Hbeta, 21–35 Hz) frequencies were selected automatically via thresholds and minimum prominence. Peaks were then visually inspected, adjusted via parameter changes or manually selected if necessary (29/658 channels in OFF and 29/651 in ON recordings). Methodological details are provided in the supplemental material and power spectra with marked peaks are available for download. Both peak occurrence, power and total power of the peak's frequency band were further analysed (see statistics) in relation to available patient characteristics including age, gender, disease duration, device (macroelectrode), clinical subtype and clinical score (UPDRS part III).

2.3. Spatial localisation of electrophysiological recording sites

Five patients were excluded from this analysis due to incomplete imaging data. In the remaining 101 patients we combined pre-operative MR-imaging and postoperative imaging data (CT- or MR-imaging) to perform electrode localisation using Lead-DBS software (Horn et al., 2019; https://www.lead-dbs.org). In short, preoperative and postoperative images were coregistered and warped into normalised space (Montreal Neurological Institute (MNI), version ICBM152 NLIN asymmetric 2009b). Electrode trajectories were automatically pre-localised from imaging artefact and manually refined when necessary. We mapped LFP recording sites to the midpoint of bipolar recording coordinates in analogy to Horn et al. (2017). Additionally, we calculated Euclidian distance (in millimetres) from the centre of recording sites to a previously defined sweet spot for clinical efficacy in STN-DBS for PD patients (Dembek et al., 2019). For visualisation and further analyses, recording sites were constrained to within 1.5 mm distance from STN. We chose not to fully limit analysis to within anatomical borders of the nucleus to retain a larger sample and since prior studies (Horn et al., 2017; Kühn et al., 2005) have shown beta extending from the dorsolateral border. Using a scattered interpolant to estimate power values in between data points, heatmaps for each frequency band were smoothed with full-width-half-maximum Gaussian kernel of 0.7 mm and visualised in MNI space with subcortical parcellations integrated in Lead-DBS (DISTAL atlas; Ewert et al., 2018) in front of a high-resolution post-mortem MRI backdrop (Edlow et al., 2019). To enhance the number of data points and for visualisation purposes, coordinates from left hemisphere were flipped non-linearly to the right.

2.4. Statistics

Comparative analyses between the group of patients with peaks and those without were performed via two-sample *t*-tests or chi-squared tests where applicable. In the case of clinical subtype's effect on spectral power, we performed one-way analysis of variance on mean power across hemispheres. Spearman correlations were used for analyses on beta power and distance to sweet spot, since data was not normally

distributed. We reported results after running randomised permutation tests with 1000 iterations with an alpha level of 0.05. Additionally, to include all data points (430 peaks/658 channels) we calculated a linear mixed effects model (LME) on log beta power (which achieved approximate normal distribution of power values) with distance to sweet spot as the fixed effect of interest and sampling site (i.e. hemisphere of each patient) as a random effect.

2.5. Data availability

Both LFP data and electrode localizations will be made available in pseudonymised fashion on a publicly accessible platform in due course after final publication of Lofredi et al. (2022). To safeguard patient privacy, we cannot provide original MRI and CT scans. Further information can be made available on request. All Matlab code included in Lead-DBS processing steps can be accessed at https://github.com/netstim/leaddbs.

3. Results

3.1. Prevalence and predictors of peaks

Analysis in the frequency domain revealed that 92% or 98 of 106 patients off medication showed at least one peak in the beta frequency band in at least one hemisphere, with 75% or 77 patients displaying peaks in both hemispheres. Overall, we found peaks in 84% or 177 of 210 hemispheres. Of the 8 patients without any beta peak, a further 5 showed peaks in the alpha band (8–12 Hz, sometimes termed "subbeta"). Co-occurrence was common, with 73 out of 98 patients with beta peaks showing alpha peaks, too. Peaks in both LBeta and Hbeta subbands were observed in 64% patients, 35% of all hemispheres and 12% of channels. An overview of peak distribution across hemispheres is provided in Fig. 1A.

In comparison to peak distribution OFF medication, the proportion of patients with peaks ON medication in LBeta band dropped markedly (75% to 50%), while HBeta peaks decreased slightly (76% to 72%). In hemispheres, the proportion of STNs with peaks in both beta bands was almost halved (37% OFF to 21% ON), while STNs presenting only HBeta peaks rose starkly (26% OFF to 42% ON). Peaks in Lbeta band were also reduced slightly (20% OFF to 16% ON), matched by an increase in STNs lacking any peak in the beta band (17% to 21%; for details, see supplemental fig. S4). Notably, alpha peak proportion in patients also diminished from 74% to 50%.

Using an alternative normalisation reference of 55–95 Hz rather than 1–100 Hz aiming to reduce the relative suppression effects from high-amplitude low-frequency activity within the reference band, peak proportions remained at similar levels, though a slight increase in Hbeta peaks, particularly ON medication, could be detected (see supplemental material incl. Fig. S1).

3.2. Frequency and power spectra

Exploring data distribution, we noticed a bimodal shape in the number of peaks recorded per frequency bin in the LBeta and HBeta bands as shown in the histogram (left y-axis) of Fig. 1B. Mean peak frequencies in the LBeta and HBeta beta bands were 16 Hz (± 2.2) and 26 Hz (± 2.7), alpha peaks centering around 9 Hz (± 1.3). Relative peak beta power plotted in the same figure (scattered dots, right y-axis) showed an exponential distribution, with higher power values at lower frequencies. The distribution was skewed (2.23).

As reported in in Lofredi et al. (2022), average power spectra across all patients revealed elevated power in the medication OFF versus ON state in both alpha and LBeta bands (Fig. 1C), significant ($p < .001$) in frequency bins from 10 to 19 Hz. Similar patterns were observed when plotting peak power around central peak frequency in each frequency band of interest (Fig. 1D).

Suppression of (higher-frequency) alpha peaks under medication has been observed in studies before (Neumann and Kühn, 2017). A subanalysis on alpha peaks and their behaviour, particularly in the absence of a low beta peak, was included in the supplement (see also S2). Results indicated that suppression at alpha frequencies of 10–12 Hz was stronger in the group presenting only alpha but not low beta peaks.

Peak beta power averaged across hemispheres correlated significantly with clinical motor score (UPDRS III; rho 0.183, p 0.037), subanalyses showing this was only true for LBeta peak power. Analysis of variance did not find a significant effect of gender (F 1.16, p 0.283), disease duration (F 1.04, p 0.437) or clinical subtype (F 1.03, p 0.362) on hemispheric average of beta power.

3.3. Patients without peaks

We compared patients with at least one beta peak (98) to those without (8), noting the asymmetry of groups. Gender proportions were skewed but not significant, with 1 out of 42 females but 7 out of 64 males lacking beta peaks ($p = .103$). All 21 tremor-dominant patients showed at least one peak, while 12% of equivalent and 8% of akinetic-rigid patients did not. We found no statistical differences between groups with regards to subtype, age, UPDRS-III score and disease duration. Only device type was a significant factor ($p = .009$). Peaks were detected in 73% of patients with Boston Scientific's directional leads compared with 95% of patients with the Medtronic and all patients with Boston Scientific's octopolar device.

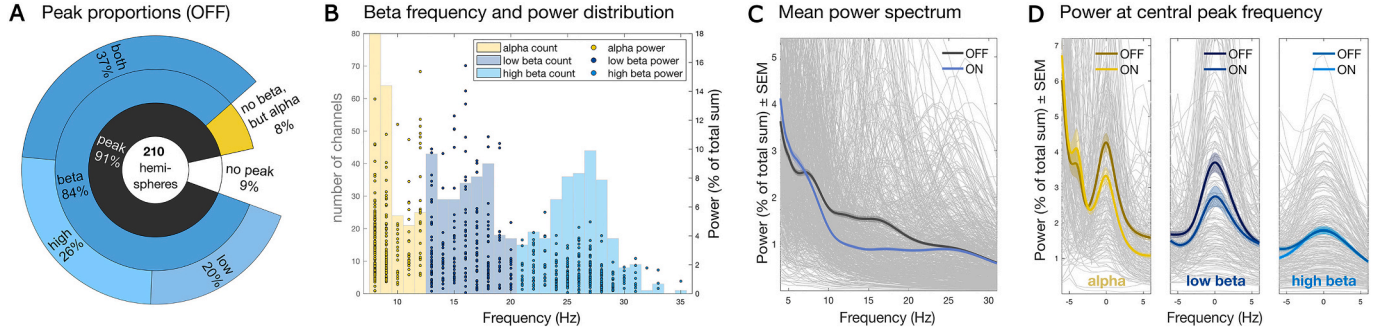

Fig. 1. A) Sunburst plot visualising the proportion of patient hemispheres ($N = 210$) with beta peaks, the latter divided into proportions of hemispheres with only LBeta, only HBeta or both within one hemisphere. Among patients without beta peaks, we also display those with alpha peaks. B) Histogram showing distribution of peak frequencies (left-y-axis) and scattered power values at each frequency (right y-axis). C) Mean power spectral density (± SEM) across hemispheres in medication OFF (N = 210) and ON ($N = 208$) states in alpha and beta frequency ranges. Mean power clearly diverges across the alpha and low beta bands. D) Mean peak power (± SEM) at central peak frequency across hemispheres are shown in colour. To demonstrate shapes of individual power spectra, all spectra are plotted in the background in dark (OFF Levodopa) and light grey (ON Levodopa).

Four of the eight patients were among the 15 patients with directional leads, where re-referencing often resulted in loss of the lowermost channel and increased movement artefact contamination further contributed to signal losses. Selective comparisons among patients with directional leads did not show striking differences between those with and those without peaks. The group with peaks averaged 1.68, those without 1.75 channels per hemisphere, compared to 2.92 channels in patients with Medtronic and 6.36 channels in patients with Boston cylindrical devices. Closest channel recording sites were about a millimeter further from the sweet spot in the directional group without peaks (3.37 ± 1.22 mm versus 2.38 ± 1.06 mm, averaged across hemispheres, n.s.).

In the other four patients without peaks, we noted a significant stun effect in two, with UPDRS OFF score at recording time significantly reduced compared to preoperative score (11 versus 19 and 10 versus 64 points), while a third patient was one of the few patients missing intra-LFP clinical scores, such that only preoperative score (31 points) was available and stun effect was unclear.

3.4. Spectral power in relation to sweet spot

On average, channels with beta peaks were 1.03 mm closer to the anatomical sweet spot compared to channels without beta peak ($p < .001$). Highest peak beta power per hemisphere showed a significant negative correlation with the distance to anatomical sweet spot (rho −0.21, p 0.006; see Fig. 2a). When split into beta subbands, HBeta but not LBeta peaks and band power negatively correlated with distance to sweet spot, both ON and OFF medication (see Fig. 2b for plots and correlation results). These results were stable after running permutation tests. Further substantiation of beta power relating to the distance from sweet spot was obtained via LME on log beta power and distance to sweet spot with patient identity and nested hemisphere as random intercepts. Fixed effects estimate was −0.154 (95% CI -0.197, −0.111, p-value 6.785×10^{12}). This demonstrated a highly significant relationship between power and distance to sweet spot. Random effects standard deviation confirmed intercept variation between patients' hemispheres (ID estimate 0.668, 95% CI 0.547, 0.817; ID:hemisphere estimate 0.380, 95% CI 0.282, 0.514). Plots of fitted versus response values and residuals are provided in the supplement (S3).

Of note, alpha peak power was not correlated with distance to anatomical sweet spot (rho 0.04, p 0.697).

3.5. Heat maps of power distribution in STN

With this large cohort of patients ($N = 106$), hemispheres ($N_{OFF} = 210$ OFF, $N_{ON} = 208$) and channels ($N_{OFF} = 658$ OFF, $N_{ON} = 651$), we had the opportunity to establish the most detailed map of the electrophysiological landscape of STN to date (Horn et al., 2017). We noted the abovementioned skewed power values and the results from the LME, where power was modulated by individual patients' hemispheres and therefore displayed data of each maximal peak per hemisphere, rather than all channels. Peak and maximal peak coordinates per hemisphere are plotted in Fig. 3a, with combined, thresholded volumetric maps of alpha and beta power, as well as LBeta and HBeta below (3b). Heat maps of all frequency bands of interest are shown separately in Fig. 3c. All beta bands (LBeta, HBeta, combined) showed very similar center of gravity (COG), whereas alpha band's COG was shifted dorso-antero-medially. In both beta bands, these data appeared to show two local maxima close to the dorsal edge, one located more rostrally and one more caudally.

4. Discussion

In postoperative rest recordings of subthalamic local field potentials we found spectral peaks in the beta frequency range in 92% of a large cohort of 106 unmedicated PD patients, irrespective of clinical subtype, patient demographics and disease severity. These results support beta peak activity as a broadly applicable feedback signal for aDBS. Secondly, we showed that peak occurrence and power (in HBeta band) were related to the distance to a target for best clinical effect or “sweet spot” for STN-DBS (Dembek et al., 2019), supporting the use of beta peak power for optimal contact selection. Heat maps of peak power within frequency bands confirmed dorso-ventral dissocation of beta and alpha bands, but showed similar distribution of LBeta and HBeta, thus supporting peak activity in both subbands as good indicators of clinically desirable, dorsolateral location within STN.

4.1. Prevalence and determinants of beta peaks

In order to implement aDBS in clinical routine, estimating the proportion of patients that show consistent beta peaks in postoperative subthalamic recordings is crucial. In our cohort, peaks were detected in 92% of PD patients and 84% of hemispheres. There was no statistical relationship between peak occurrence and patient age, gender, disease duration, subtype and clinical score, though due to the small number ($N = 8$) of patients without peaks, these results were somewhat limited. Issues such as incomplete OFF state and missing channels might have contributed to lack of peaks in several of these patients.

The directional device was significantly overrepresented in the patients without peaks, though this was most likely due to recording and referencing methodology, resulting in fewer channels per hemisphere. Our laboratory notes experience with lower signal-to-noise ratio of recordings from these macroelectrodes, related to wiring configuration

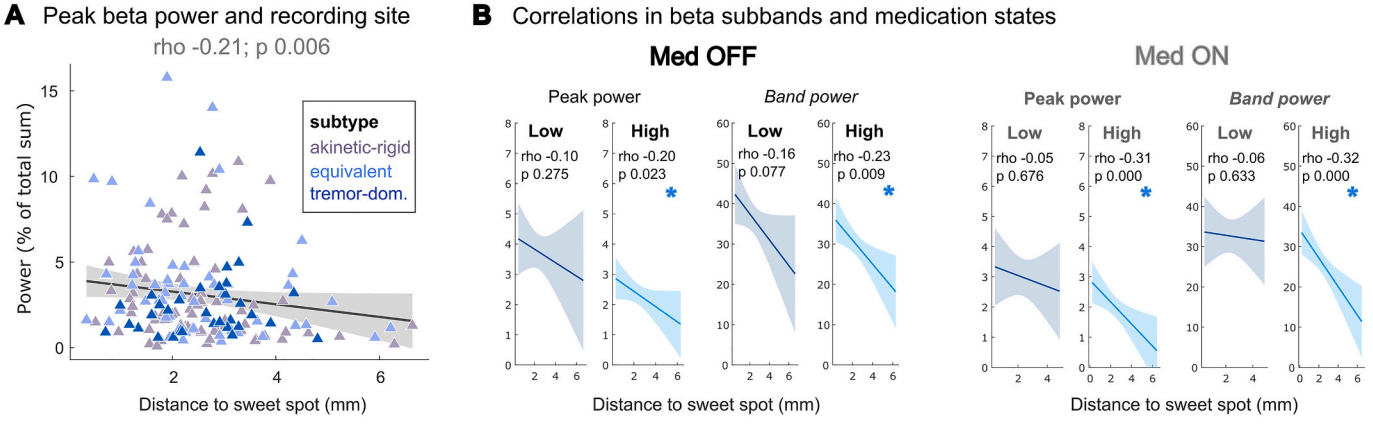

Fig. 2. A) Scattered peak power values from channels with highest peak per hemisphere in the medication OFF state correlated with their distance to clinical sweet spot (see methods). Colours denote clinical subtypes, showing a wide variety of power values in all three subtypes. B) Data from A is split into LBeta and HBeta beta peaks and band power in the left panel. In the right panel, analogous correlations were performed for the LFP data recorded when patients were ON medication.

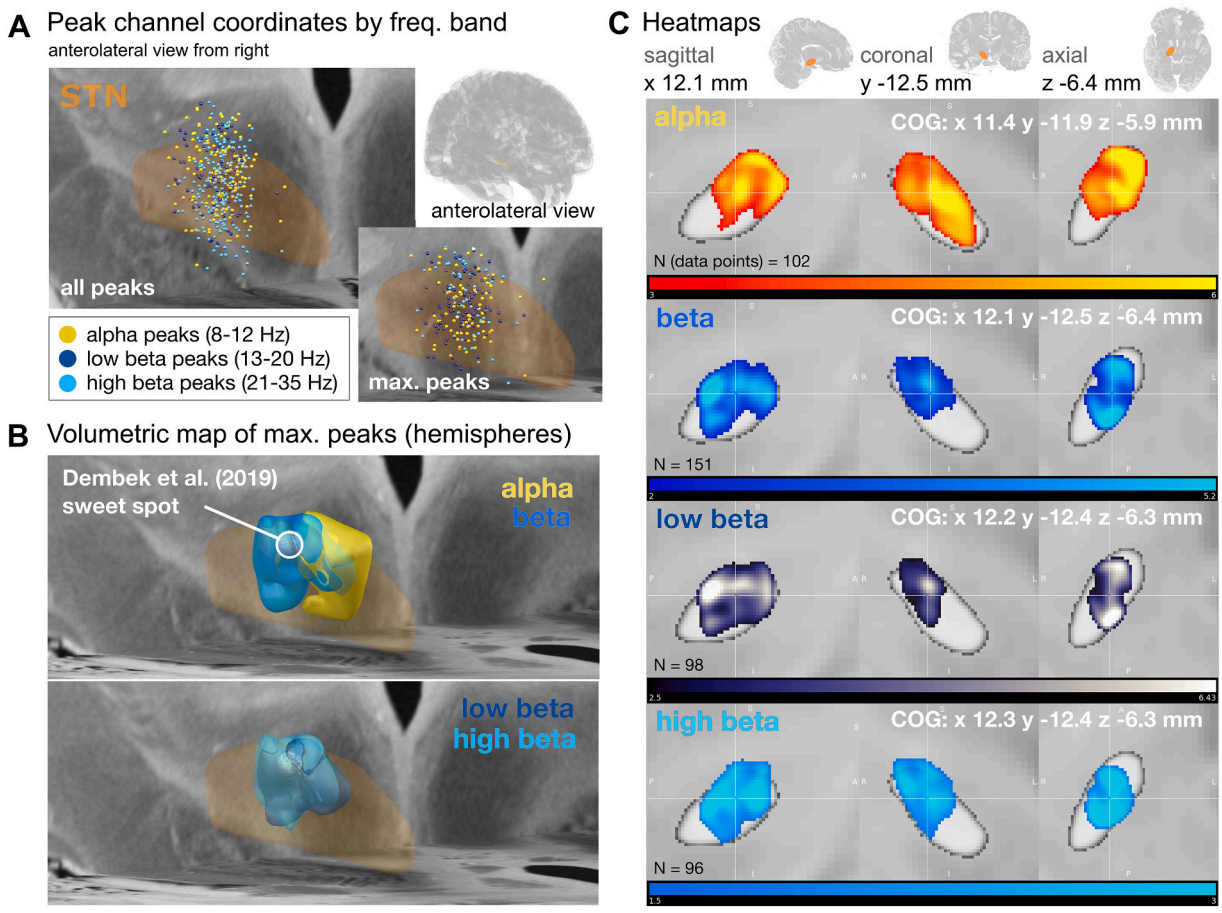

Fig. 3. Power distribution of frequency bands in anatomical space. A) Peak coordinates scattered in MNI space colour-coded by frequency band, view from anterolateral right. Upper right: transparent brain showing perspective. Upper left: all beta ($N = 407$) and alpha peaks ($N = 199$), lower right only maximal peaks per hemisphere (151 beta and 102 alpha peaks). B) Volumetric map of power distribution to visualise proximity and overlap of different frequency bands. The sweet spot for clinical effect used for correlation analyses is plotted as a white 1 mm sphere (x 12.50 y − 12.72 z − 5.38). C) Heat maps in 3D slices for each frequency band with colormap and thresholds. Lighter colours indicating higher power values. All plots are set to the center of gravity (COG) of the beta band for comparability (see crosshairs). The number of data points for each heatmap is noted.

and proneness to movement artefacts. The sample size of patients with these leads (15 out of 106) was quite small. Future studies including larger samples and multiple manufacturers of increasingly adopted directional devices will hopefully elucidate the matter further.

Though previous reports did not find tremor scores correlated with beta activity (Neumann and Kühn, 2017; Zaidel et al., 2010), all 21 tremor-dominant patients in this cohort showed at least one reliable peak in the beta range. This held true in most hemispheres, too (88.1%). With a mean clinical score of UPDRS 31.4 points, we presume that these patients also exhibited some akinetic-rigid symptoms, which have been shown (von Coelln et al., 2021) to develop in patients with longer disease durations (mean: 9.6 years). Future studies may do well to include clinical subscores or more detailed clinical phenomenology into their analyses.

Our study further revealed a reduction in the proportion of patients with peaks ON medication, decreasing by roughly a third in the LBeta and alpha bands, but only marginally in HBeta band.

As discussed in the limitations below, the postoperative stun effect in this cohort may have reduced proportion and particularly power of beta peak activity. Therefore, beta band activity may increase with time when the stun effect wears off. There are limited data available on long term recordings using chronic sensing devices (Anderson et al., 2021; Chen et al., 2020) or LFP recorded during exchange of the pulse generator (Abosch et al., 2012; Giannicola et al., 2012). These studies have mostly shown stability of the beta band activity over time, including the postoperative time point (Neumann et al., 2017), and robust response to high-frequency stimulation (Giannicola et al., 2012). Accessible chronic recordings via novel devices have recently been adopted by researchers successfully (Arlotti et al., 2021; Feldmann et al., 2022; van Rheede et al., 2022; Thenaisie et al., 2021) such that we can expect far more data on this matter in the near future.

4.2. *Spectral power in patients, frequency bands and dopaminergic states*

Peak power values varied considerably between patients and hemispheres, as well as between individual frequencies and frequency bands (see Figs. 1c, 2a). The number of peaks per frequency bin in this cohort indicated a bimodal distribution within the beta band, splitting it into LBeta and HBeta "subbands". This coincides with an ongoing debate on the nature of these subbands, which present variation in clinical phenomenology (Neuville et al., 2021; Singh et al., 2013) and therapeutic modulation: as in this study, differences have been shown regarding effects from medication (Neumann et al., 2016; Priori et al., 2004) and also by neuromodulation (Blumenfeld et al., 2017; Chen et al., 2020), both within STN and in the wider cortico-basal ganglia network (Brittain and Brown, 2014) e.g. in long-range phase-amplitude coupling (van Wijk et al., 2016).

In line with previous studies (Brown et al., 2001; Oswal et al., 2016; Priori et al., 2004), activity in LBeta (and alpha) band correlated with clinical score in this cohort (Lofredi et al., 2022). This would suggest

favouring LBeta, reflective of symptom severity, as the more useful feedback signal to guide adaptive algorithms. However, the use of MDS-UPDRS score for symptom severity may omit specific symptoms which relate to other biomarkers (Godinho et al., 2021; Khawaldeh et al., 2021; Toledo et al., 2014). Nevertheless, HBeta's relative robustness with regard to medication and the stun effect (see fig. 4a in Rosa et al., 2010, noting differences in band definitions) might be advantageous for guiding parameter and contact selection in routine clinical settings.

4.3. Spatial power distribution in relation to clinical target and within STN

Our results demonstrated a negative correlation between the distance from recording site to clinical target and beta peak power. This is in line with a study on intraoperative microelectrode trajectory recordings, that found clinically active macroelectrodes to coincide with the centre of dorsolateral oscillatory region within STN (Zaidel et al., 2010). Split into subbands, only HBeta power was significantly correlated with distance to anatomical sweet spot for clinical effect. On medication the HBeta correlation prevailed, in line with the subbands relative resilience under the influence of Levodopa. Importantly, this implicates HBeta as a potential biomarker both for contact selection as well as in aDBS paradigms in clinical routine when treating medicated patients. Whether DBS itself selectively decreases either of the beta subbands cannot be determined from these data. Regarding long-term DBS effects, one study showed consistent suppression of both subbands over 6 months and interestingly suggested early (1-month-postop) symptom-relevant frequency suppression in HBeta band, which shifted into LBeta band at 3 and 6 months postop (Chen et al., 2020).

We stratified peak power distribution in frequency bands of interest within and around 210 STNs. Heat maps of power in the frequency bands of interest replicated dorsolateral distribution of beta power, as previously shown in microelectrode recordings (Kühn et al., 2005; Trottenberg et al., 2007) as well as the more anteromedial concentration of alpha power (Horn et al., 2017). Notably, heatmaps in the two beta subbands were highly similar with adjacent centers of gravity (see Figs. 3b,c).

In summary, these results support the use of HBeta as an electrophysiological signature for the dorsolateral STN, both for intraoperative target selection as well as for contact programming, both postoperatively as well as under the influence of medication. LBeta, a superior marker of symptom severity, showed highly similar anatomical distribution to HBeta, implying that stimulation at sites of peak HBeta oscillatory activity will likely overlap with LBeta regions.

4.4. Limitations

We believe that a central limitation of this study, the postoperative stun effect at implantation site, might play a role in the discrepant correlation results between beta subbands. The swelling of newly damaged tissue (microlesion effect) is known to alleviate motor symptoms both intraoperatively and for several days after implantation without active DBS (Chen et al., 2006; Singh et al., 2012). This might have decreased particularly LBeta power around the implanted region in some patients, leading to less reliable information in this subband, though one study showed LBeta power returning to baseline 48 h after implantation (Rosa et al., 2010). Secondly, recordings were performed in a bipolar fashion with a distance of 2 mm between the centres of neighbouring contacts. To measure differences in electrical potential, one of the contacts must be outside the “oscillator”. If both poles are within a site of synchronised activity, the potential difference will be zero. In a study that measured the length of dorsolateral oscillatory region of STN, most extended beyond 2 mm (see Fig. 2 in Zaidel et al., 2010). This too might account for the seemingly reduced power amplitude in the centre of the beta heatmaps giving the impression of two local maxima. Different methods of recording electrophysiological activity e.g. monopolar recordings or use of phase reversal (Rodriguez-Oroz et al., 2011) can contribute to this matter in future studies, though they bear their own limitations. Finally, this study analysed rest recordings under laboratory conditions that revealed beta activity as a consistent biomarker in the vast majority of patients off medication. In order to use beta activity as a feedback marker for aDBS, effects of medication, movement as well as other potential artefacts induced by activities of daily living need to be considered.

Further, we note the method of power normalisation in this study, reporting percentage of total sum of power across a wide frequency range. Even so, comparability of this relative power between subjects remains limited, since variation in other frequency bands, particularly low frequencies with high power values following $1/f^N$ distribution (Bédard and Destexhe, 2009) change amplitudes in the frequency band of interest. Controlling for low frequency modulation by normalisation to a narrower, high frequency band (55–95 Hz), in a supplemental examination, we did indeed observe a slight increase in Hbeta peaks. Though these methods limit power-related within- and between-subject results, they should have fewer implications for most current clinical applications, since these typically employ individualised approaches with patient-specific power thresholds in a narrow frequency band.

On a general note, the field of invasive subcortical recordings commonly relies on historical EEG terminology when describing spectral activity, which can be very helpful for backwards comparability, especially in the context of brain networks encompassing cortical regions but is neither universally defined nor based on solid physiological foundations. Indeed, both ours and past studies (Neumann and Kühn, 2017) have shown peaks in higher-frequency alpha band that mimic low beta peaks in their behaviour under medication (and stimulation). Future studies may do well to consider more flexible approaches.

5. Conclusion

Overall, we found spectral peaks in the beta band in subthalamic LFP recordings to be highly prevalent in the largest cohort of PD patients to date. It was a reliably detectable biomarker in a PD cohort representing a broad clinical spectrum, allowing widespread recommendation of beta-guided parameter selection and adaptive DBS algorithms. With regards to beta subbands, we conclude that even in immediately postoperative patients, peak power in high beta band is both a good marker of location (with similar anatomical distribution to LBeta within STN) and more reliable in medicated patients. We therefore propose that at early stages of programming as well as in effectively medicated patients, contacts with peaks in this frequency band can be chosen to steer programming settings e.g. contact configuration. Peak frequencies in LBeta band, which more accurately represent symptom severity, can be incorporated at later stages, particularly in demand-related peak-guided aDBS algorithms.

Financial disclosure

ND, RL, BA, CB and JH report no conflicts of interest. PK reports personal fees from Medtronic and Stadapharm, outside the submitted work. GHS reports personal fees from Medtronic, Boston Scientific and Abbott, outside the submitted work. AK reports personal fees from Medtronic, Boston Scientific, Abbott, Ipsen Pharma and Teva outside the submitted work.

Funding sources

Dr. Darcy and Dr. Lofredi are partly funded by the (Junior) Clinician Scientist Program funded by the Charité – Universitätsmedizin Berlin and the Berlin Institute of Health at Charité (BIH). The work was supported by Deutsche Forschungsgemeinschaft (Project-ID 424778381 – TRR 295 Retune).

CRediT authorship contribution statement

Natasha Darcy: Conceptualization, Formal analysis, Methodology, Visualization, Writing – original draft. **Roxanne Lofredi:** Conceptualization, Data curation, Investigation, Methodology, Supervision, Writing – review & editing. **Bassam Al-Fatly:** Formal analysis, Visualization, Writing – review & editing. **Wolf-Julian Neumann:** Investigation. **Julius Hübl:** Investigation. **Christof Brücke:** Investigation. **Patricia Krause:** Investigation. **Gerd-Helge Schneider:** Resources. **Andrea Kühn:** Conceptualization, Resources, Methodology, Supervision, Writing – review & editing.

Declaration of Competing Interest

Dr. Darcy, Dr. Lofredi, Mr. Al-Fatly, Dr. Brücke and Dr. Hübl report no conflicts of interest. Dr. Krause reports personal fees from Medtronic and Stadapharm, outside the submitted work. Dr. Schneider reports personal fees from Medtronic, Boston Scientific and Abbott, outside the submitted work. Prof. Kühn reports personal fees from Medtronic, Boston Scientific, Abbott, Ipsen Pharma and Teva outside the submitted work.

Appendix A. Supplementary data

Supplementary data to this article can be found online at https://doi.org/10.1016/j.expneurol.2022.114150.

References

Abosch, A., Lanctin, D., Onaran, I., Eberly, L., Spaniol, M., Ince, N.F., 2012. Long-term recordings of local field potentials from implanted deep brain stimulation electrodes. Neurosurgery 71, 804–814. https://doi.org/10.1227/neu.0b013e3182676b91.

Anderson, R.W., Kehnemouyi, Y.M., Neuville, R.S., Wilkins, K.B., Anidi, C.M., Petrucci, M.N., Parker, J.E., Velisar, A., Brontë-Stewart, H.M., 2020. A novel method for calculating beta band burst durations in Parkinson's disease using a physiological baseline. J. Neurosci. Methods 343, 108811. https://doi.org/10.1016/j.jneumeth.2020.108811.

Anderson, R.W., Wilkins, K.B., Parker, J.E., Petrucci, M.N., Kehnemouyi, Y., Neuville, R. S., Cassini, D., Trager, M.H., Koop, M.M., Velisar, A., Blumenfeld, Z., Quinn, E.J., Henderson, J., Bronte-Stewart, H.M., 2021. Lack of progression of beta dynamics after long-term subthalamic neurostimulation. Ann Clin Transl Neur 8, 2110–2120. https://doi.org/10.1002/acn3.51463.

Arlotti, M., Rossi, L., Rosa, M., Marceglia, S., Priori, A., 2016. An external portable device for adaptive deep brain stimulation (aDBS) clinical research in advanced Parkinson's disease. Med. Eng. Phys. 38, 498–505. https://doi.org/10.1016/j.medengphy.2016.02.007.

Arlotti, M., Marceglia, S., Foffani, G., Volkmann, J., Lozano, A.M., Moro, E., Cogiamanian, F., Prenassi, M., Bocci, T., Cortese, F., Rampini, P., Barbieri, S., Priori, A., 2018. Eight-hours adaptive deep brain stimulation in patients with Parkinson disease. Neurology 90, e971–e976. https://doi.org/10.1212/wnl.0000000000005121.

Arlotti, M., Colombo, M., Bonfanti, A., Mandat, T., Lanotte, M.M., Pirola, E., Borellini, L., Rampini, P., Eleopra, R., Rinaldo, S., Romito, L., Janssen, M.L.F., Priori, A., Marceglia, S., 2021. A new implantable closed-loop clinical neural Interface: first application in Parkinson's disease. Front. Neurosci. 15, 763235 https://doi.org/10.3389/fnins.2021.763235.

Bédard, C., Destexhe, A., 2009. Macroscopic models of local field potentials and the apparent 1/f noise in brain activity. Biophys. J. 96, 2589–2603. https://doi.org/10.1016/j.bpj.2008.12.3951.

Blumenfeld, Z., Koop, M.M., Prieto, T.E., Shreve, L.A., Velisar, A., Quinn, E.J., Trager, M. H., Brontë-Stewart, H., 2017. Sixty-hertz stimulation improves bradykinesia and amplifies subthalamic low-frequency oscillations. Mov. Disord. 32, 80–88. https://doi.org/10.1002/mds.26837.

Brittain, J.-S., Brown, P., 2014. Oscillations and the basal ganglia: motor control and beyond. Neuroimage 85, 637–647. https://doi.org/10.1016/j.neuroimage.2013.05.084.

Bronte-Stewart, H.M., Petrucci, M.N., O'Day, J.J., Afzal, M.F., Parker, J.E., Kehnemouyi, Y.M., Wilkins, K.B., Orthlieb, G.C., Hoffman, S.L., 2020. Perspective: evolution of control variables and policies for closed-loop deep brain stimulation for Parkinson's disease using bidirectional deep-brain-computer interfaces. Front. Hum. Neurosci. 14, 353. https://doi.org/10.3389/fnhum.2020.00353.

Brown, P., 2003. Oscillatory nature of human basal ganglia activity: Relationship to the pathophysiology of Parkinson's disease. Mov. Disord. 18, 357–363. https://doi.org/10.1002/mds.10358.

Brown, P., Oliviero, A., Mazzone, P., Insola, A., Tonali, P., Lazzaro, V.D., 2001. Dopamine dependency of oscillations between subthalamic nucleus and pallidum in Parkinson's disease. J. Neurosci. 21, 1033–1038. https://doi.org/10.1523/jneurosci.21-03-01033.2001.

Cassidy, M., Mazzone, P., Oliviero, A., Insola, A., Tonali, P., Lazzaro, V.D., Brown, P., 2002. Movement-related changes in synchronization in the human basal ganglia. Brain 125, 1235–1246. https://doi.org/10.1093/brain/awf135.

Chen, C.C., Pogosyan, A., Zrinzo, L.U., Tisch, S., Limousin, P., Ashkan, K., Yousry, T., Hariz, M.I., Brown, P., 2006. Intra-operative recordings of local field potentials can help localize the subthalamic nucleus in Parkinson's disease surgery. Exp. Neurol. 198, 214–221. https://doi.org/10.1016/j.expneurol.2005.11.019.

Chen, Y., Gong, C., Tian, Y., Orlov, N., Zhang, J., Guo, Y., Xu, S., Jiang, C., Hao, H., Neumann, W.-J., Kühn, A.A., Liu, H., Li, L., 2020. Neuromodulation effects of deep brain stimulation on beta rhythm: a longitudinal local field potential study. Brain Stimul 13, 1784–1792. https://doi.org/10.1016/j.brs.2020.09.027.

Deffains, M., Iskhakova, L., Katabi, S., Israel, Z., Bergman, H., 2018. Longer β oscillatory episodes reliably identify pathological subthalamic activity in parkinsonism. Mov. Disord. 33, 1609–1618. https://doi.org/10.1002/mds.27418.

Dembek, T.A., Roediger, J., Horn, A., Reker, P., Oehrn, C., Dafsari, H.S., Li, N., Kühn, A. A., Fink, G.R., Visser-Vandewalle, V., Barbe, M.T., Timmermann, L., 2019. Probabilistic sweet spots predict motor outcome for deep brain stimulation in Parkinson disease. Ann. Neurol. 86, 527–538. https://doi.org/10.1002/ana.25567.

Edlow, B.L., Mareyam, A., Horn, A., Polimeni, J.R., Witzel, T., Tisdall, M.D., Augustinack, J.C., Stockmann, J.P., Diamond, B.R., Stevens, A., Tirrell, L.S., Folkerth, R.D., Wald, L.L., Fischl, B., van der Kouwe, A., 2019. 7 tesla MRI of the ex vivo human brain at 100 micron resolution. Sci Data 6, 244. https://doi.org/10.1038/s41597-019-0254-8.

Ewert, S., Plettig, P., Li, N., Chakravarty, M.M., Collins, D.L., Herrington, T.M., Kühn, A. A., Horn, A., 2018. Toward defining deep brain stimulation targets in MNI space: a subcortical atlas based on multimodal MRI, histology and structural connectivity. Neuroimage 170, 271–282. https://doi.org/10.1016/j.neuroimage.2017.05.015.

Feldmann, L.K., Lofredi, R., Neumann, W.-J., Al-Fatly, B., Roediger, J., Bahners, B.H., Nikolov, P., Denison, T., Saryyeva, A., Krauss, J.K., Faust, K., Florin, E., Schnitzler, A., Schneider, G.-H., Kühn, A.A., 2022. Toward therapeutic electrophysiology: beta-band suppression as a biomarker in chronic local field potential recordings. Npj Park Dis 8, 44. https://doi.org/10.1038/s41531-022-00301-2.

Giannicola, G., Rosa, M., Servello, D., Menghetti, C., Carrabba, G., Pacchetti, C., Zangaglia, R., Cogiamanian, F., Scelzo, E., Marceglia, S., Rossi, L., Priori, A., 2012. Subthalamic local field potentials after seven-year deep brain stimulation in Parkinson's disease. Exp. Neurol. 237, 312–317. https://doi.org/10.1016/j.expneurol.2012.06.012.

Gilron, R., Little, S., Perrone, R., Wilt, R., de Hemptinne, C., Yaroshinsky, M.S., Racine, C. A., Wang, S.S., Ostrem, J.L., Larson, P.S., Wang, D.D., Galifianakis, N.B., Bledsoe, I. O., Luciano, M.S., Dawes, H.E., Worrell, G.A., Kremen, V., Borton, D.A., Denison, T., Starr, P.A., 2021. Long-term wireless streaming of neural recordings for circuit discovery and adaptive stimulation in individuals with Parkinson's disease. Nat. Biotechnol. 39, 1078–1085. https://doi.org/10.1038/s41587-021-00897-5.

Godinho, F., Neto, A.F., Bianqueti, B.L., Luccas, J.B., Varjão, E., Filho, P.R.T., Figueiredo, E.G., Almeida, T.P., Yoneyama, T., Takahata, A.K., Rocha, M.S., Soriano, D.C., 2021. Spectral characteristics of subthalamic nucleus local field potentials in Parkinson's disease: phenotype and movement matter. Eur. J. Neurosci. 53, 2804–2818. https://doi.org/10.1111/ejn.15103.

Guidetti, M., Marceglia, S., Loh, A., Harmsen, I.E., Meoni, S., Foffani, G., Lozano, A.M., Moro, E., Volkmann, J., Priori, A., 2021. Clinical perspectives of adaptive deep brain stimulation. Brain Stimul 14, 1238–1247. https://doi.org/10.1016/j.brs.2021.07.063.

Hoang, K.B., Cassar, I.R., Grill, W.M., Turner, D.A., 2017. Biomarkers and stimulation algorithms for adaptive brain stimulation. Front. Neurosci. 11, 564. https://doi.org/10.3389/fnins.2017.00564.

Horn, A., Neumann, W., Degen, K., Schneider, G., Kühn, A.A., 2017. Toward an electrophysiological "sweet spot" for deep brain stimulation in the subthalamic nucleus. Hum. Brain Mapp. 38, 3377–3390. https://doi.org/10.1002/hbm.23594.

Horn, A., Li, N., Dembek, T.A., Kappel, A., Boulay, C., Ewert, S., Tietze, A., Husch, A., Perera, T., Neumann, W.-J., Reisert, M., Si, H., Oostenveld, R., Rorden, C., Yeh, F.-C., Fang, Q., Herrington, T.M., Vorwerk, J., Kühn, A.A., 2019. Lead-DBS v2: towards a comprehensive pipeline for deep brain stimulation imaging. Neuroimage 184, 293–316. https://doi.org/10.1016/j.neuroimage.2018.08.068.

Jimenez-Shahed, J., 2021. Device profile of the percept PC deep brain stimulation system for the treatment of Parkinson's disease and related disorders. Expert Rev Med Devic 18, 1–14. https://doi.org/10.1080/17434440.2021.1909471.

Khawaldeh, S., Tinkhauser, G., Torrecillos, F., He, S., Foltynie, T., Limousin, P., Zrinzo, L., Oswal, A., Quinn, A.J., Vidaurre, D., Tan, H., Litvak, V., Kühn, A., Woolrich, M., Brown, P., 2021. Balance between competing spectral states in subthalamic nucleus is linked to motor impairment in Parkinson's disease. Brain 145, 237–250. https://doi.org/10.1093/brain/awab264.

Krauss, J.K., Lipsman, N., Aziz, T., Boutet, A., Brown, P., Chang, J.W., Davidson, B., Grill, W.M., Hariz, M.I., Horn, A., Schulder, M., Mammis, A., Tass, P.A., Volkmann, J., Lozano, A.M., 2021. Technology of deep brain stimulation: current status and future directions. Nat. Rev. Neurol. 17, 75–87. https://doi.org/10.1038/s41582-020-00426-z.

Kühn, A.A., Williams, D., Kupsch, A., Limousin, P., Hariz, M., Schneider, G., Yarrow, K., Brown, P., 2004. Event-related beta desynchronization in human subthalamic nucleus correlates with motor performance. Brain 127, 735–746. https://doi.org/10.1093/brain/awh106.

Kühn, A.A., Trottenberg, T., Kivi, A., Kupsch, A., Schneider, G.-H., Brown, P., 2005. The relationship between local field potential and neuronal discharge in the subthalamic

nucleus of patients with Parkinson's disease. Exp. Neurol. 194, 212–220. https://doi.org/10.1016/j.expneurol.2005.02.010.

Kühn, A.A., Kupsch, A., Schneider, G., Brown, P., 2006. Reduction in subthalamic 8–35 Hz oscillatory activity correlates with clinical improvement in Parkinson's disease. Eur. J. Neurosci. 23, 1956–1960. https://doi.org/10.1111/j.1460-9568.2006.04717.x.

Kühn, A.A., Kempf, F., Brücke, C., Doyle, L.G., Martinez-Torres, I., Pogosyan, A., Trottenberg, T., Kupsch, A., Schneider, G.-H., Hariz, M.I., Vandenberghe, W., Nuttin, B., Brown, P., 2008. High-frequency stimulation of the subthalamic nucleus suppresses oscillatory β activity in patients with Parkinson's disease in parallel with improvement in motor performance. J. Neurosci. 28, 6165–6173. https://doi.org/10.1523/jneurosci.0282-08.2008.

Kühn, A.A., Tsui, A., Aziz, T., Ray, N., Brücke, C., Kupsch, A., Schneider, G.-H., Brown, P., 2009. Pathological synchronisation in the subthalamic nucleus of patients with Parkinson's disease relates to both bradykinesia and rigidity. Exp. Neurol. 215, 380–387. https://doi.org/10.1016/j.expneurol.2008.11.008.

Kühn, A., Tonder, L., Raike, R., Stanslaski, S., Lynch, K., Bronte-Stewart, H., 2020. Adaptive DBS algorithm for personalized therapy in Parkinson's disease: ADAPT-PD trial: A prospective single-blind, randomized crossover, multi-center trial of deep brain stimulation adaptive algorithms in subjects with Parkinson's disease. In: Parkinson's disease: Clinical trials, movement disorders [abstract]. Presented at the MDS Virtual Congress 2020, Movement Disorders.

Little, S., Pogosyan, A., Neal, S., Zavala, B., Zrinzo, L., Hariz, M., Foltynie, T., Limousin, P., Ashkan, K., FitzGerald, J., Green, A.L., Aziz, T.Z., Brown, P., 2013. Adaptive deep brain stimulation in advanced Parkinson disease. Ann. Neurol. 74, 449–457. https://doi.org/10.1002/ana.23951.

Lofredi, R., Tan, H., Neumann, W.-J., Yeh, C.-H., Schneider, G.-H., Kühn, A.A., Brown, P., 2019. Beta bursts during continuous movements accompany the velocity decrement in Parkinson's disease patients. Neurobiol. Dis. 127, 462–471. https://doi.org/10.1016/j.nbd.2019.03.013.

Lofredi, R., Okudzhava, L., Irmen, F., Brücke, C., Huebl, J., Krauss, J.K., Schneider, G.-H., Faust, K., Neumann, W.-J., Kühn, A.A., 2022. Subthalamic beta bursts correlate with dopamine-dependent motor symptoms in 106 Parkinson's patients. Biorxiv. https://doi.org/10.1101/2022.05.06.490913, 2022.05.06.490913.

Marceglia, S., Conti, C., Svanidze, O., Foffani, G., Lozano, A.M., Moro, E., Volkmann, J., Arlotti, M., Rossi, L., Priori, A., 2022. Double-blind cross-over pilot trial protocol to evaluate the safety and preliminary efficacy of long-term adaptive deep brain stimulation in patients with Parkinson's disease. BMJ Open 12, e049955. https://doi.org/10.1136/bmjopen-2021-049955.

Nakajima, A., Shimo, Y., Fuse, A., Tokugawa, J., Hishii, M., Iwamuro, H., Umemura, A., Hattori, N., 2021. Case report: chronic adaptive deep brain stimulation personalizing therapy based on parkinsonian state. Front. Hum. Neurosci. 15, 702961 https://doi.org/10.3389/fnhum.2021.702961.

Neumann, W., Kühn, A.A., 2017. Subthalamic beta power—unified Parkinson's disease rating scale III correlations require akinetic symptoms. Mov. Disord. 32, 175–176. https://doi.org/10.1002/mds.26858.

Neumann, W.-J., Degen, K., Schneider, G.-H., Brücke, C., Huebl, J., Brown, P., Kühn, A. A., 2016. Subthalamic synchronized oscillatory activity correlates with motor impairment in patients with Parkinson's disease: correlation of subthalamic B oscillations and PD symptoms. Mov. Disord. 31, 1748–1751. https://doi.org/10.1002/mds.26759.

Neumann, W.-J., Staub-Bartelt, F., Horn, A., Schanda, J., Schneider, G.-H., Brown, P., Kühn, A.A., 2017. Long term correlation of subthalamic beta band activity with motor impairment in patients with Parkinson's disease. Clin. Neurophysiol. 128, 2286–2291. https://doi.org/10.1016/j.clinph.2017.08.028.

Neuville, R.S., Petrucci, M.N., Wilkins, K.B., Anderson, R.W., Hoffman, S.L., Parker, J.E., Velisar, A., Bronte-Stewart, H.M., 2021. Differential effects of pathological Beta burst dynamics between Parkinson's disease phenotypes across different movements. Front. Neurosci. 15, 733203 https://doi.org/10.3389/fnins.2021.733203.

Oostenveld, R., Fries, P., Maris, E., Schoffelen, J.-M., 2011. FieldTrip: open source software for advanced analysis of MEG, EEG, and invasive electrophysiological data. Comput Intel Neurosc 2011, 156869. https://doi.org/10.1155/2011/156869.

Oswal, A., Beudel, M., Zrinzo, L., Limousin, P., Hariz, M., Foltynie, T., Litvak, V., Brown, P., 2016. Deep brain stimulation modulates synchrony within spatially and spectrally distinct resting state networks in Parkinson's disease. Brain 139, 1482–1496. https://doi.org/10.1093/brain/aww048.

Piña-Fuentes, D., van Dijk, J.M.C., van Zijl, J.C., Moes, H.R., van Laar, T., Oterdoom, D.L. M., Little, S., Brown, P., Beudel, M., 2020. Acute effects of adaptive deep brain stimulation in Parkinson's disease. Brain Stimul 13, 1507–1516. https://doi.org/10.1016/j.brs.2020.07.016.

Prenassi, M., Arlotti, M., Borellini, L., Bocci, T., Cogiamanian, F., Locatelli, M., Rampini, P., Barbieri, S., Priori, A., Marceglia, S., 2021. The relationship between electrical energy delivered by deep brain stimulation and levodopa-induced Dyskinesias in Parkinson's disease: a retrospective preliminary analysis. Front. Neurol. 12, 643841 https://doi.org/10.3389/fneur.2021.643841.

Priori, A., Foffani, G., Pesenti, A., Tamma, F., Bianchi, A.M., Pellegrini, M., Locatelli, M., Moxon, K.A., Villani, R.M., 2004. Rhythm-specific pharmacological modulation of subthalamic activity in Parkinson's disease. Exp. Neurol. 189, 369–379. https://doi.org/10.1016/j.expneurol.2004.06.001.

Rodriguez-Oroz, M.C., López-Azcárate, J., Garcia-Garcia, D., Alegre, M., Toledo, J., Valencia, M., Guridi, J., Artieda, J., Obeso, J.A., 2011. Involvement of the subthalamic nucleus in impulse control disorders associated with Parkinson's disease. Brain 134, 36–49. https://doi.org/10.1093/brain/awq301.

Rosa, M., Marceglia, S., Servello, D., Foffani, G., Rossi, L., Sassi, M., Mrakic-Sposta, S., Zangaglia, R., Pacchetti, C., Porta, M., Priori, A., 2010. Time dependent subthalamic local field potential changes after DBS surgery in Parkinson's disease. Exp. Neurol. 222, 184–190. https://doi.org/10.1016/j.expneurol.2009.12.013.

Rosa, M., Arlotti, M., Marceglia, S., Cogiamanian, F., Ardolino, G., Fonzo, A.D., Lopiano, L., Scelzo, E., Merola, A., Locatelli, M., Rampini, P.M., Priori, A., 2017. Adaptive deep brain stimulation controls levodopa-induced side effects in parkinsonian patients. Mov. Disord. 32, 628–629. https://doi.org/10.1002/mds.26953.

Sharott, A., Gulberti, A., Zittel, S., Jones, A.A.T., Fickel, U., Münchau, A., Köppen, J.A., Gerloff, C., Westphal, M., Buhmann, C., Hamel, W., Engel, A.K., Moll, C.K.E., 2014. Activity parameters of subthalamic nucleus neurons selectively predict motor symptom severity in Parkinson's disease. J. Neurosci. 34, 6273–6285. https://doi.org/10.1523/jneurosci.1803-13.2014.

Singh, A., Kammermeier, S., Mehrkens, J.H., Bötzel, K., 2012. Movement kinematic after deep brain stimulation associated microlesions. J. Neurol. Neurosurg. Psychiatry 83, 1022. https://doi.org/10.1136/jnnp-2012-302309.

Singh, A., Plate, A., Kammermeier, S., Mehrkens, J.H., Ilmberger, J., Bötzel, K., 2013. Freezing of gait-related oscillatory activity in the human subthalamic nucleus. Basal Ganglia 3, 25–32. https://doi.org/10.1016/j.baga.2012.10.002.

Thenaisie, Y., Palmisano, C., Canessa, A., Keulen, B.J., Capetian, P., Jiménez, M.C., Bally, J.F., Manferlotti, E., Beccaria, L., Zutt, R., Courtine, G., Bloch, J., van der Gaag, N.A., Hoffmann, C.F., Moraud, E.M., Isaias, I.U., Contarino, M.F., 2021. Towards adaptive deep brain stimulation: clinical and technical notes on a novel commercial device for chronic brain sensing. J. Neural Eng. 18, 042002 https://doi.org/10.1088/1741-2552/ac1d5b.

Tinkhauser, G., Pogosyan, A., Tan, H., Herz, D.M., Kühn, A.A., Brown, P., 2017. Beta burst dynamics in Parkinson's disease OFF and ON dopaminergic medication. Brain 140, 2968–2981. https://doi.org/10.1093/brain/awx252.

Toledo, J.B., López-Azcárate, J., Garcia-Garcia, D., Guridi, J., Valencia, M., Artieda, J., Obeso, J., Alegre, M., Rodriguez-Oroz, M., 2014. High beta activity in the subthalamic nucleus and freezing of gait in Parkinson's disease. Neurobiol. Dis. 64, 60–65. https://doi.org/10.1016/j.nbd.2013.12.005.

Trottenberg, T., Kupsch, A., Schneider, G.-H., Brown, P., Kühn, A.A., 2007. Frequency-dependent distribution of local field potential activity within the subthalamic nucleus in Parkinson's disease. Exp. Neurol. 205, 287–291. https://doi.org/10.1016/j.expneurol.2007.01.028.

van Rheede, J.J., Feldmann, L.K., Busch, J.L., Fleming, J.E., Mathiopoulou, V., Denison, T., Sharott, A., Kühn, A.A., 2022. Diurnal modulation of subthalamic beta oscillatory power in Parkinson's disease patients during deep brain stimulation. Medrxiv. https://doi.org/10.1101/2022.02.09.22270606, 2022.02.09.22270606.

van Wijk, B.C.M., Beudel, M., Jha, A., Oswal, A., Foltynie, T., Hariz, M.I., Limousin, P., Zrinzo, L., Aziz, T.Z., Green, A.L., Brown, P., Litvak, V., 2016. Subthalamic nucleus phase–amplitude coupling correlates with motor impairment in Parkinson's disease. Clin. Neurophysiol. 127, 2010–2019. https://doi.org/10.1016/j.clinph.2016.01.015.

Velisar, A., Syrkin-Nikolau, J., Blumenfeld, Z., Trager, M.H., Afzal, M.F., Prabhakar, V., Bronte-Stewart, H., 2019. Dual threshold neural closed loop deep brain stimulation in Parkinson disease patients. Brain Stimul 12, 868–876. https://doi.org/10.1016/j.brs.2019.02.020.

von Coelln, R., Gruber-Baldini, A.L., Reich, S.G., Armstrong, M.J., Savitt, J.M., Shulman, L.M., 2021. The inconsistency and instability of Parkinson's disease motor subtypes. Parkinsonism Relat D 88, 13–18. https://doi.org/10.1016/j.parkreldis.2021.05.016.

Weinberger, M., Mahant, N., Hutchison, W.D., Lozano, A.M., Moro, E., Hodaie, M., Lang, A.E., Dostrovsky, J.O., 2006. Beta oscillatory activity in the subthalamic nucleus and its relation to dopaminergic response in Parkinson's disease. J. Neurophysiol. 96, 3248–3256. https://doi.org/10.1152/jn.00697.2006.

Whitmer, D., de Solages, C., Hill, B., Yu, H., Henderson, J.M., Bronte-Stewart, H., 2012. High frequency deep brain stimulation attenuates subthalamic and cortical rhythms in Parkinson's disease. Front. Hum. Neurosci. 6, 155. https://doi.org/10.3389/fnhum.2012.00155.

Zaidel, A., Spivak, A., Grieb, B., Bergman, H., Israel, Z., 2010. Subthalamic span of β oscillations predicts deep brain stimulation efficacy for patients with Parkinson's disease. Brain 133, 2007–2021. https://doi.org/10.1093/brain/awq144.